Article

Energy and Exergy Analysis of Different Exhaust Waste Heat Recovery Systems for Natural Gas Engine Based on ORC

Guillermo Valencia [1], Armando Fontalvo [2], Yulineth Cárdenas [3], Jorge Duarte [1] and Cesar Isaza [4]

[1] Departamento de Ingeniería Mecánica, Universidad del Atlántico, Carrera 30 Número 8-49, Puerto Colombia, Barranquilla 080007, Colombia; guillermoevalencia@mail.uniatlantico.edu.co (G.V.); jorgeduarte@mail.uniatlantico.edu.co (J.D.)

[2] School of Computer Science and Engineering, The Australian National University, ACT 2601, Australia; armando.fontalvo@anu.edu.au

[3] Departamento de Energía, Universidad de la Costa, Barranquilla 080002, Colombia; ycardena6@cuc.edu.co

[4] Programa de Ingeniería Mecánica, Universidad Pontificia Bolivariana, Medellín 050004, Colombia; cesar.isaza@upb.edu.co

- Correspondence: guillermoevalencia@mail.uniatlantico.edu.co; Tel.: +575-324-94-31

Abstract: One way to increase overall natural gas engine efficiency is to transform exhaust waste heat into useful energy by means of a bottoming cycle. Organic Rankine cycle (ORC) is a promising technology to convert medium and low grade waste heat into mechanical power and electricity. This paper presents an energy and exergy analysis of three ORC-Waste heat recovery configurations by using an intermediate thermal oil circuit: Simple ORC (SORC), ORC with Recuperator (RORC) and ORC with Double Pressure (DORC), and Cyclohexane, Toluene and Acetone have been proposed as working fluids. An energy and exergy thermodynamic model is proposed to evaluate each configuration performance, while available exhaust thermal energy variation under different engine loads was determined through an experimentally validated mathematical model. Additionally, the effect of evaportating pressure on net power output , absolute thermal efficiency increase, absolute specific fuel consumption decrease, overall energy conversion efficiency, and component exergy destruction is also investigated. Results evidence an improvement in operational performance for heat recovery through RORC with Toluene at an evaporation pressure of 3.4 MPa, achieving 146.25 kW of net power output, 11.58% of overall conversion efficiency, 28.4% of ORC thermal efficiency, and an specific fuel consumption reduction of 7.67% at a 1482 rpm engine speed, a 120.2 L/min natural gas Flow, 1.784 lambda, and 1758.77 kW mechanical engine power.

Keywords: Energy analysis; exergy analysis; organic Rankine cycle; waste heat recovery; natural gas engine.

1. Introduction

The technological advances developed in organic Rankine cycles (ORC) applied to waste heat recovery (WHR) systems could become a promising feature for the engine manufacturing industry due to its capacity to reduce fuel consumption, increase net power output, and reduce greenhouse gas emissions [1].

ORCs are now considered as a feasible tool to increase the energy efficiency due to the heat recovery capacity of alternative sources, such as exhaust gases, cooling water or lubricating oil, and the use of organic and environmentally friendly working fluids [2]. Furthermore, ORCs allow their configuration to vary at different levels of complexity considering the temperature of the heat source, in order to achieve the highest possible thermodynamic performance [3].

During the installation of an ORC in the exhaust line of an engine, several safety hazards must be considered due to the possible contact of the exhaust gases with the organic working fluid.

Furthermore, the overall system performance must be verified due to the increase in weight of the component and the power consumption in the engine under counterpressure conditions [4].

The first record of an ORC application was developed by Parimal S. Patell and Edward F. Doyle in 1976, in which they propose to recover the energy from exhaust gases in a Mack 676 diesel vehicle engine, to obtain a 13% more power with the same fuel consumption [5]. Additionally, B. Peris et al. present the results in simulations of waste heat recovery from the cooling water process and not from the exhaust gases of Internal Combustion Engines (ICE) of six ORC configurations working with ten non-flammable fluids [6].

Approaching in energy optimization, G. Yu et al. developed a simulation model based on the actual behavior of a diesel engine, with the aim of waste heat recovery from both the engine exhaust gases and cooling water, using as R245fa as working fluid. The results evidence that approximately 75% of the residual heat of the exhaust gases, and 9,5% of the residual heat of the cooling water can be recovered under specific operating conditions, additionally, the operating conditions of the recovery cycle must be optimized in order to maintain the power output [7]. However, these results are limited to an exergetic analysis of a single ORC configuration.

Yiji Lu et al. integrate a SORC and solids adsorption technology with a 152 kW ICE diesel, for the recovery of heat generated in the cooling system and exhaust gases from the power cycle. From the results obtained in their research, it is possible to design the working conditions for a cogeneration system, where the maximum recoverable power from the cooling process and exhaust systems are 67,9 kW and 82.7,kW respectively. While assembling to a cogeneration system can provide an output power of 13,9 kW and cooling power of 16,6 kW in nominal engine conditions [8], these results reveal the feasibility of recovery processes from waste gases by reducing specific fuel consumption, without including exergetic or thermo-economic studies.

Several researches have been directed towards the optimization of combined cycle power plants and households. R. Chacartegui et al. studied only the low temperature SORC configuration in medium and large-scale combined cycle plants, with the purpose of evaluating the performance of high-efficiency gas turbines rather than gas-fired generation engines, working with organic fluids such as R-113, R-245, isobutene, toluene, cyclohexane and isopentane, where favorable results were obtained for the combined ORC cycles of toluene and cyclohexane [9]. The scope of the study was focused on an energy analysis with economic considerations without a thermo-economic approach. Moreover, K Qiu et al. experimentally examined the integration of a thermoelectric generation system with a small amount of output power of 1 kW, with a dual ORC, to verify the performance of energy generation, under representative conditions of the system [10].

During a period time from 2007 to 2010, authors such as Drescher et al. [11] researched new working fluids in ORC for biomass applications. Meanwhile, Mago et al. [12] theoretically studied the effect that these fluids have on the performance of ORC at different operating temperatures and pressures. Kosmadakis et al. [13] performed tests on more than 30 organic fluids, in this study, it was determined the R245fa as the most suitable organic fluid for ORC applications with ICE in terms of performance, however, in environmental area, its use is restricted by international standards given its global warming potential (GWP) value. For solar applications, Tchance et al. [14] determined that the most suitable fluid is the refrigerant R-134a, due to its low toxicity and flammability, in addition to the high ratio of pressure and efficiency that can be handled in the ORC when used.

For a time frame since 2010 until 2013, several contributions were made to the application of ORC in power generation plants with biomass and combustion engines, highlighting the work of Vaja and Gambarotta [15], through the evaluation of the performance of the SORC and RORC configurations, from the energy and non-thermal-economic point of view. For the heat recovery from waste gases of a stationary ICE of 2900 kW, it was achieved a 12% of the increase in the overall

efficiency of the system. The system was evaluated for a single operating condition of the thermal source, without the inclusion of economic indicators in order to determine the viability of the proposed system. Kalina [16], investigated the performance of a biomass electric power generation plant composed of a gasifier, two gas ICE G3412C LE and G3412C TA of 360 kW and 280 kW respectively, and an ORC, the latter was used as a heat recovery system for the waste gases of the engine and cooling water. The theoretical study falls short of experimental results of the thermal source and economic analysis to prove and guarantee its feasibility and viability in a real-life context. Mingshanet al. [17] performed a first-law analysis for a SORC configuration in order to recover exhaust energy from a heavy-duty diesel engine. It was determined that the system has a heat recovery efficiency between 10% and 15% when the heat exchanger is optimized. Furthermore, the engine operates under partial load conditions with a medium-high power condition instead of the nominal operative point of the engine. Therefore the variation in the operating speeds of the engine must be evaluated, which requires a robust model of the engine to be evaluated.

Tian et al. [18] then performed a techno-economic analysis of a single ORC assembled to a 235 kW diesel ICE, with the purpose to evaluate 20 different working fluids and obtain significant results such as the highest net output power per unit of mass flow and the highest energy efficiency with refrigerants R-141b and R-123 respectively. The study was limited to a single engine operating condition and a proposal for parametric optimization of the generation cost and evaporator dimensions.

In the period from 2013 to 2015, academic researches were focused on developing ORC heat recovery systems for solar thermal and geothermal power generation applications. Highlighting the work of Hung et al [19] who investigated the behavior of the SORC, only for the recovery of energy from the residual heat of the air produced by solar ventilation systems, consequently, the overall efficiency of the system increased by 6.2%. On the other hand, Zare V. [20] began to evaluate economic criteria for thermal performance studies applied to three ORC configurations associated with binary geothermal power plants. Results indicated that the RORC presents better performance in thermal efficiency, while, the SORC displayed better results in economic indicators, due to the fact that it consists of the least amount of equipment and the acquisition cost is lower. The results are limited only to the geothermal source evaluated, and the working fluids studied, in addition, the analysis of the DORC was not presented in this research.

Additionally, several researches focusing on the second law of thermodynamics have been developed, without thermo-economic analysis such as the modeling developed by Kerme and Orfi [21], who evaluate the effect of the input temperature of an ORC turbine on the main parameters of energy and exergetic efficiency driven by solar collectors. As a result, was obtained that the net electrical efficiency is directly related to the increase in the input temperature of the system, contrary to the total exergy destruction rate, which is inversely proportional to the input temperature in the system. As a result, for an ORC it must be considered to present optimal operating parameters and mainly comply with the criterion of minimum destroyed exergy. The exergetic analysis permits to identify every feature that directly affects the overall energy efficiency, and the calculation of the exergo economic costs, which aims to set an economic value for materials and energy flows, providing a reasonable base for the allocation of economic resources [22].

This work aims to promote the rational use of energy and the preservation of the environment by increasing the energy efficiency of the Jenbacher JMS 612 GS-N. L natural gas engine of 2 MW, by taking advantage of the waste heat of the exhaust gases, using the configurations of SORC and RORC, through different organic working fluids such as toluene, cyclohexane, and acetone, selected due to their thermodynamic performance and environmental considerations. The conservation of natural resources, the limited availability of spaces to generate energy through some renewable sources, cost savings, policies and the national regulatory framework are some of the most important factors that

encourage the research of a more efficient energy generation process for internal combustion engines [23].

2. Methodology

2.1 Description of the system

This section presents a general description of the 2 MW natural gas generation engine and the two configurations of ORC WHR systems with indirect heating. The physical structure of each configuration is presented with a detailed description of considered operating principle, as well as the energy and exergy balances applied to the modeling of the WHR systems studied including the validation of these models.

The engine considered to evaluate the WHR system is the Jenbacher JMS 612 GS-N. L of 12 cylinders as shown in Figure 1 which has the capacity to operate at a minimum load of 1000 kW, with lambda of 1.79 and maximum load of 1982 kW with lambda of 1.97, emitting waste exhaust gases with concentrations ranging from 9.45% to 10.52% of O_2, 731 mg/m^3 to 588 mg/m^3 of CO, 461 mg/m^3 to 468 mg/m^3 of NOx, 317 mg/m^3 to 368 mg/m^3 of NO_2, and 95 mg/m^3 to 65 mg/m^3 of NO.

Figure 1. Jenbacher JMS-612 GS-N. L electric generation engine

The physical parameters of the engine are summarized in Table 1. The composition of the fuel used in the plastic production plant studied is mainly 97.97% CH_4, 1.5% N_2, 0.25% C_2H_6 and 0.16% CO_2, which mixture with air is given at a line pressure between 1.15 bar and 1.21 bar, and an uncorrected volumetric ratio of 110 L/s to 140 L/s so that to obtain an optimum flammable gas-air mixture and an exhaust gas with a temperature after the expander of the turbocharger ranging from 420 °C to 460 °C.

Table 1. Physical parameters of Jenbacher JMS 612 GS-N. L engine

Description	Value	Units
Cylinder capacity	74,852	L
Compression ratio	10,5	
Number of cylinders	12	$In\ V\ 60°$
Stroke length	220	mm
Diameter in chamber	190	mm
Maximum torque	60,66	$kN \times m$
Maximum power	1820	$kW@1500rpm$
Nominal speed	1500	rpm
Ignition system	Spark ignition	

2.2 Description of the SORC, RORC, and DORC.

The configurations studied are presented in Figure 2 [24]. The physical structure for the SORC is shown as in Figure 2a; this structure operates as follows: an air-natural gas mixture (stream 1) is supplied to the ICE, which is compressed (stream 6) to mixing conditions prior to enter in the combustion chamber. The exhaust gases at the outlet of the manifold (stream 9) expand in the expansion stage of the turbocharger up to stream 10, which are evacuated to the environment (stream 11) after transferring the energy in the shell and tube heat exchanger (ITC 1), with the thermal oil (stream 3 AT) that circulates through the secondary circuit of coupling employing the energy supplied by Pump 1 (B 1). The hot thermal oil (stream 1 AT) serves as a thermal source to evaporate the organic fluid to reach the superheated steam phase (1 ORC) at the high pressure and temperature from the ORC to the turbine (T 1). The heat transfer process in ITC 2 is carried out in three zones called preheating (Zone 1), evaporation (Zone 2) and superheating (Zone 3). As the organic fluid in the turbine (T 1) from the evaporator (ITC 2) expands, an energy conversion process occurs in the generator (G). The expansion of the fluid is given until the low pressure to enter the condenser (ITC 3), where all the mass is condensed until reaching the saturated liquid phase (stream 3 ORC). The condensation process takes place in two stages that have been called condensation (stream 1 A – stream 1g A) and cooling (stream 1g A – stream 2 A). Subsequently, in the pump (B 2), the fluid is taken to the evaporating pressure in the ITC 2 exchanger, thus, completing the heat recovery system through a SORC cycle.

The heat recovery system operating in the SORC configuration with heat exchanger shown in Figure 2b consists of four heat exchange units: a shell and tube heat exchanger (ITC 1), an evaporator (ITC 2), a condenser (ITC 3) and a heat recovery unit (RC), additionally the secondary circuit coupling pump (B 1), the organic fluid pump (B 2) and a turbine (T 1). In this configuration, it is possible to achieve an improvement in efficiency when the high-temperature organic fluid at the turbine outlet (T 1) (1 ORC stream) preheats the organic fluid through the recuperator (RC) before reaching the evaporator (ITC 2). The pump (B 2) transports the fluid to the high cycle pressure (5 ORC stream), this is in order to be supplied to all components of the system. Subsequently, the organic fluid is evaporated in the ITC 2 exchanger, which is composed by three zones, to complete the thermodynamic cycle of power recovery [25], [26], [27].

The ORC cycle with two evaporating pressures shown in Figure 2c consists of two evaporators (ITC 2 - ITC 4) and one condenser (ITC 3), two pumps (B 2-B 3), and two turbines (T 1 - T 2). During this process, the organic fluid enters the second stage of the turbine (T 2) as superheated steam at high pressure and temperature from the evaporator (ITC 4), where it expands to the intermediate operating pressure of the pump (B 2). Consequently, the fluid enters the second stage in the turbine

(T 1) expanding to a mixture of the low operating pressure of the condenser, where the fluid cools down to the liquid phase. Afterwards, the pump (B 2) discharges the intermediate pressure of the cycle, so that a fraction of it evaporates in the ITC 2 exchanger and mixes with the current from the T2 turbine, while the remaining fraction enters the B3 pump where it is taken to the high pressure of the cycle to evaporate in the ITC 4 exchanger, finally completing the Rankine cycle of two evaporating pressures. This configuration increases the efficiency of the cycle by decreasing the thermal load dissipated to the environment [28].

Preprints (www.preprints.org) | NOT PEER-REVIEWED | Posted: 20 May 2019 doi:10.20944/preprints201905.0247.v1

Peer-reviewed version available at Energies 2019, 12, 2378; doi:10.3390/en12122378

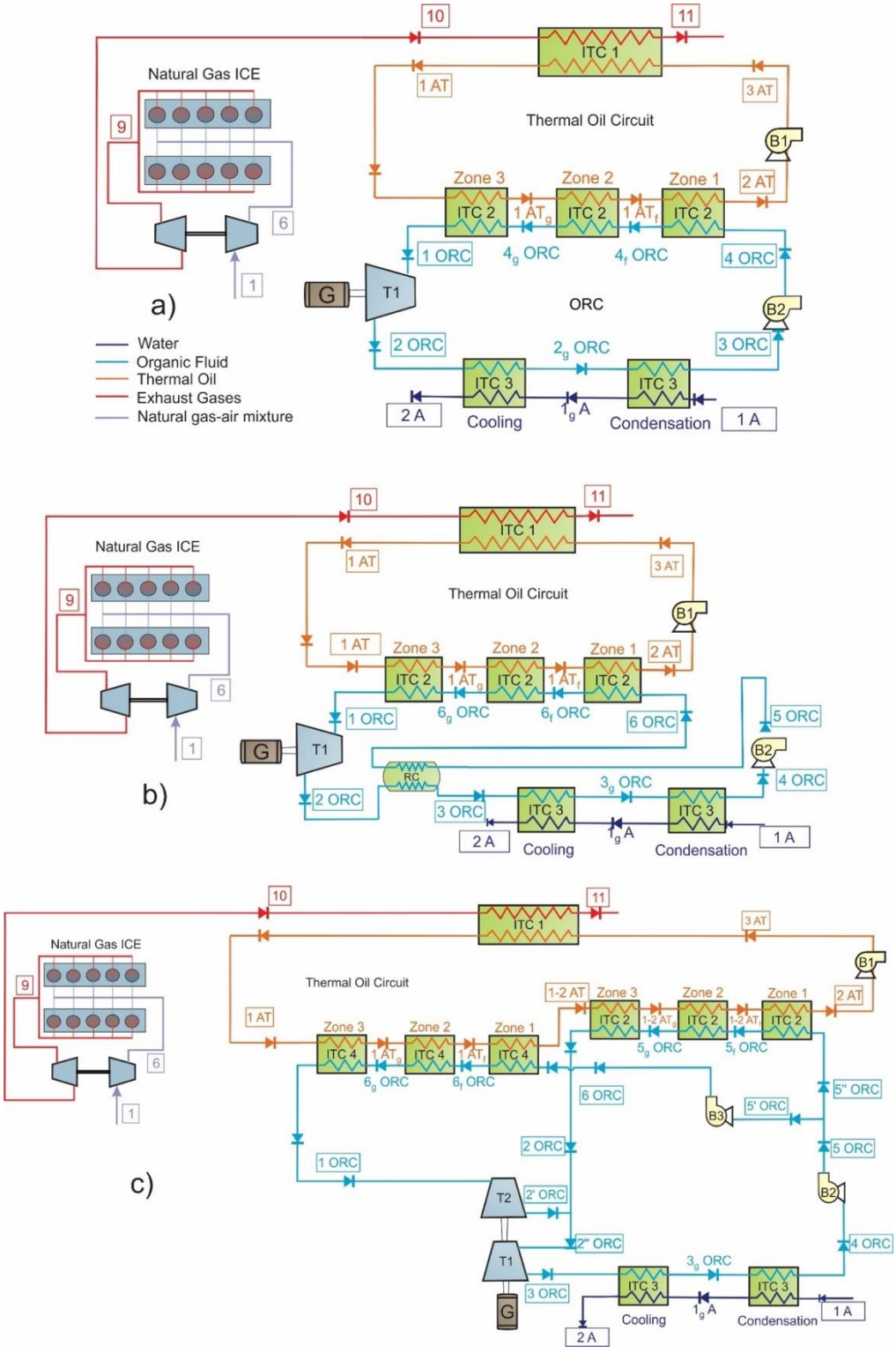

Figure 2. Physical structure of the WHR system, a) SORC, b) RORC and c) DORC

3. Thermodynamic modeling

For this specific study of every WHR system, it is presented an energy analysis conducted by applying the first law of thermodynamics to each of the components of the system. It also presents the definition of Fuel - Product for each component of the three configurations under study, in

addition to the performance indicators of each configuration through the first and second law of thermodynamics.

3.1 Energy analysis

Every single component of the ORC recovery systems was considered to be volume control systems operating in a steady state. The mass balance as in Equation 1 and the energy balance as in Equation 2 were applied to each component.

$$\sum \dot{m}_{in} - \sum \dot{m}_{out} = \frac{dm}{dt}, \tag{1}$$

$$\sum \dot{m}_{in} h_{in} - \sum \dot{m}_{out} h_{out} - \sum \dot{Q} + \sum \dot{W} = \frac{dE}{dt}, \tag{2}$$

where m and E represent the mass and energy contained in the control volume respectively, $\dot{m}$ is the organic fluid mass flow, h the specific enthalpy, $\dot{Q}$ the heat flow and $\dot{W}$ the power.

3.2 Exergetic analysis

The specific exergy for each of the process states, as opposed to the exhaust gases, was calculated by neglecting the variation of kinetic and potential energy, resulting as shown in Equation 3.

$$ex = (h - h_0) - T_0(s - s_0), \tag{3}$$

where enthalpy h_0, and entropy s_0 of the current are calculated at the reference conditions of 298.15 K and 101.3 kPa. The chemical exergy of the exhaust gases product of combustion (stream 10), is defined considering a mixture of gases, a product of the combustion of natural gas. The chemical exergy of the gas mixture is given as in Equation 4.

$$ex_G^{ch} = \sum_{i=1}^{n} X_i ex^{ch_i} + RT_0 \sum_{i=1}^{n} X_i \ln X_i, \tag{4}$$

where R represents the universal constant of the gases, and X_i the molar fraction of the gas, and the term ex^{ch_i} per mol of each gas.

From the calculated exergies, the exergy balance was made to each component of the proposed configurations using Equation 5 [29].

$$\sum \dot{m}_{in} ex_{in} - \sum \dot{m}_{out} ex_{out} + \dot{Q}\left(1 - \frac{T_0}{T}\right) - \dot{W} - \dot{E}x_D = \frac{dEx_{VC}}{dt} \tag{5}$$

where $\dot{m}_{in} ex_{in}$ refers to the exergy flow of the input stream, and $\dot{m}_{out} ex_{out}$ to the exergy flow of the output stream of each component, $\dot{E}x_D$ is the term related to the destruction of exergy in the component, while $\frac{dEx_{VC}}{dt}$ represents the variation of the exergy of the system over time.

Three energy indicators are studied with the purpose to evaluate the performance of the WHR systems: cycle thermal efficiency ($\eta_{I,c}$), heat recovery efficiency (ε_{hr}), and overall energy conversion efficiency ($\eta_{I,global}$) [30]. The cycle thermal efficiency is calculated by means of Equation 6, and represents the net output ratio of power of the heat recovery system with ORC $\dot{W}_{neto}$ to the heat recovered from the engine exhaust.

$$\eta_{I,C} = \frac{\dot{W}_{neto}}{\dot{Q}_G}. \quad (6)$$

The heat recovery efficiency calculated through Equation 7, represents the amount of heat recovered from the exhaust gases concerning their maximum thermal availability. Whereas the overall energy conversion efficiency calculated as in Equation 8, relates the net output power to the available heat in the exhaust gases.

$$\varepsilon_{hr} = \frac{\dot{Q}_G}{\dot{m}_{10} C_{P10} (T_{10} - T_0)} \quad (7)$$

$$\eta_{I,overall} = \eta_{I,C} * \varepsilon_{hr}. \quad (8)$$

Similarly, the absolute increase in thermal efficiency is calculated using Equation 9, which relates the net power generated by the heat recovery system through an ORC configuration to the energy provided by the fuel. This indicator determines the improvement in the performance of an ICE with a given heat recovery system.

$$\Delta\eta_{thermic} = \frac{\dot{W}_{neto}}{\dot{m}_{fuel} \times LHV} \quad (9)$$

Due to the additional power supply with the heat recovery system over the engine power, there is a lower specific fuel consumption (BSFC) which is determined by Equation 10 [31].

$$BSFC_{ORC-engine} = \frac{m_{fuel}}{\dot{W}_{engine} + \dot{W}_{neto}}. \quad (10)$$

furthermore, the absolute decrease in specific fuel consumption is determined by Equation 11 and represents a reduction in fuel consumption for particular operating conditions of the power generation engine.

$$\Delta BSFC = \frac{\left|BSFC_{ORC-engine} - BSFC_{engine}\right|}{BSFC_{engine}} * 100. \quad (11)$$

The exergy efficiency based on the second law of thermodynamics ($\eta_{II,ORC}$) is now calculated as in Equation 12.

$$\eta_{II,ORC} = \frac{\dot{E}x_{produced}}{\dot{E}x_{supplied}}, \quad (12)$$

where $\dot{E}x_{supplied}$ is the amount of exergy supplied to the system, and $\dot{E}x_{produced}$ the exergy produced by the system. Exergetic efficiency can be expressed as a function of the destroyed exergy $\dot{E}_D$ through Equation 13.

$$\eta_{II,ORC} = 1 - \frac{\dot{E}x_D}{\dot{E}x_{supplied}} \quad (13)$$

3.3 *Exergy analysis*

In order to construct a thermodynamic model for each configuration of the proposed recovery systems, the following assumptions, that govern the phenomenology of the process and delimit the scope of the results obtained, were considered:

- Pressure drops in pipes are neglected, whereas in heat exchange equipment the pressure drop is considered as a function of the geometry and hydraulic characteristics of the flow.

- All the components of the cycle are thermally insulated.
- The variation in exhaust gas temperature is compensated by the thermal oil flow in the thermal coupling cycle, ensuring that the ORC studied work under steady state conditions.

The energy and exergetic analysis of each of the three proposed ORC configurations were developed in Matlab R2018b® [32], environment, calculating the thermodynamic properties in each of the process states with the REFPROP 8.0® [33].

A specific operating condition of the Jenbacher JMS 612 GS-N L engine was selected so that it can be possible to compare the results of the proposed configurations, whose operating parameters considered for simulation are shown in Table 2. A particular operating condition of the process and was selected for this study due to the fact that it contains representative values of the operation of the system when it operates in an off-grid mode independent of the network.

Table 2. Parameters considered for ICE simulation

Parameter	Value	Units
Gas flow	120	L/min
Lambda	1,784	
Rpm	1482	rev/min
Gas pressure	1163,6	$mbar$
Throttle valve	80	%
Turbo bypass valve	9,1	%
Gas temperature	389	°C
Engine coolant temperature	63,9	°C

The performance indicators of the engine in the selected base operating condition are shown in Table 3, which are expected to be evaluated with each of the configurations.

Table 3. Performance indicators for ICE

Performance Indicators	Value	Units
Mechanical engine power	1758,77	kW
Effective engine efficiency	38,59	%
Heat recovery efficiency	40,78	%
Heat removed from exhaust gases	514,85	kW
Specific engine fuel consumption	177,65	g/kWh

The parameters considered for the study of WHR systems are shown as in

Table **4**.

Preprints (www.preprints.org) | NOT PEER-REVIEWED | Posted: 20 May 2019 doi:10.20944/preprints201905.0247.v1

Peer-reviewed version available at Energies 2019, 12, 2378; doi:10.3390/en12122378

Table 4. Parameters considered for proposed configurations

Configuration	Parameter	Value	Units	Reference
S / R / DP	Isentropic efficiency turbines	80	%	[34]
S / R / DP	Isentropic efficiency pumps	75	%	[34]
S / R / DP	Cooling water temperature (T1A)	50	°C	
S / R / DP	Pinch Point condenser (ITC3)	15	°C	
S / R	Pressure Ratio B1	2,5		
DP	Pressure Ratio B1	11,09		
S / R / DP	Pinch Point evaporators (ITC2) (ITC4)	35	°C	
R	Recovery Effectiveness (RC)	85	%	[34]
DP	Pressure Ratio B2	20		
DP	Pressure Ratio B3	9		
S / R	Pressure Ratio B2	30		

The detailed equations of the energy balance applied to each component of the proposed configurations are shown in Appendix A, Table A.13.

Accordingly, for each component can be differentiated an input, a product, a destroyed exergy value, in some cases the exergy loss must be differentiated from the exergy destroyed [35]. The Input-output structure for the components of the proposed WHR systems is shown as in Table 5.

Table 5. Fuel-Product definition for each configuration

Component	Different configurations of waste heat recovery systems using ORC								
	SORC			RORC			DORC		
	Fuel	Product	Lost	Fuel	Product	Lost	Fuel	Product	Lost
ITC1	$\dot{E}_{x10}$ $\dot{E}_{x11}$	$\dot{E}_{x1AT}$ - $\dot{E}_{x3AT}$		$\dot{E}_{10}$	$\dot{E}_{1AT}$-$\dot{E}_{3AT}$	$\dot{E}_{11}$	$\dot{E}_{x10}$	$\dot{E}_{x1AT}$-$\dot{E}_{x3AT}$	$\dot{E}_{x11}$
B1	$\dot{W}_{B1}$	$\dot{E}_{x3AT}$-$\dot{E}_{x2AT}$	-	$\dot{W}_{B1}$	$\dot{E}_{x3AT}$-$\dot{E}_{x2AT}$	-	$\dot{W}_{B1}$	$\dot{E}_{x3AT}$-$\dot{E}_{x2AT}$	-
ITC2	$\dot{E}_{x1AT}$-$\dot{E}_{x2AT}$	$\dot{E}_{x1ORC}$- $\dot{E}_{x4ORC}$	-	$\dot{E}_{x1AT}$-$\dot{E}_{x2AT}$	$\dot{E}_{x1ORC}$-$\dot{E}_{x6ORC}$	-	$\dot{E}_{x1-2AT}$- $\dot{E}_{x2AT}$	$\dot{E}_{x2ORC}$-$\dot{E}_{x5ORC}$	-
T1	$\dot{E}_{x1ORC}$-$\dot{E}_{x2ORC}$	$\dot{W}_{T1}$	-	$\dot{E}_{x1ORC}$- $\dot{E}_{x2ORC}$	$\dot{W}_{T1}$	-	$\dot{E}_{x2,,ORC}$ - $\dot{E}_{x3}$	$\dot{W}_{T1}$	-
ITC3	- $\dot{E}_{2A}$		-	- $\dot{E}_{2A}$		-	- $\dot{E}_{2A}$		-
B2	$\dot{W}_{B2}$	$\dot{E}_{x4ORC}$- $\dot{E}_{x3ORC}$	-	$\dot{W}_{B2}$	$\dot{E}_{x5ORC}$-$\dot{E}_{x4ORC}$	-	$\dot{W}_{B2}$	$\dot{E}_{x5ORC}$-$\dot{E}_{x4ORC}$	-
RC	-	-		$\dot{E}_{x2ORC}$-$\dot{E}_{x3ORC}$	$\dot{E}_{x6ORC}$-$\dot{E}_{x5ORC}$	-	-	-	
T2	-	-		-	-		$\dot{E}_{x1ORC}$-$\dot{E}_{x2,ORC}$	$\dot{W}_{T2}$	-
B3	-	-		-	-		$\dot{W}_{B3}$	$\dot{E}_{x6ORC}$ -$\dot{E}_{x5ORC}$	-
ITC4	-	-		-	-		$\dot{E}_{x1AT}$-$\dot{E}_{x1-2AT}$	$\dot{E}_{x1ORC}$-$\dot{E}_{x6ORC}$	-

3.4 *Validation*

To validate the SORC configuration model, a comparative analysis was conducted with the results of research performed by [36], [37]. The main parameters considered for both investigations are shown in **Table 6**.

Table 6. Data used from the system for model validation

η_B	η_T	T_{fuente} [ºC]	F [kg/s]	T_{Cond} [ºC]	Pinch Point [ºC]	P_{Vap} [Mpa]
0,8	0,7	250	2,737	35	30	0,8-5,5

This model was validated considering two working fluids, R-11 and R-134a. Based on the conditions reported in Table 6, the thermal efficiencies of the system were determined as a function of the Turbine inlet pressure. The results of the behavior obtained for both fluids are shown in Figure 3.

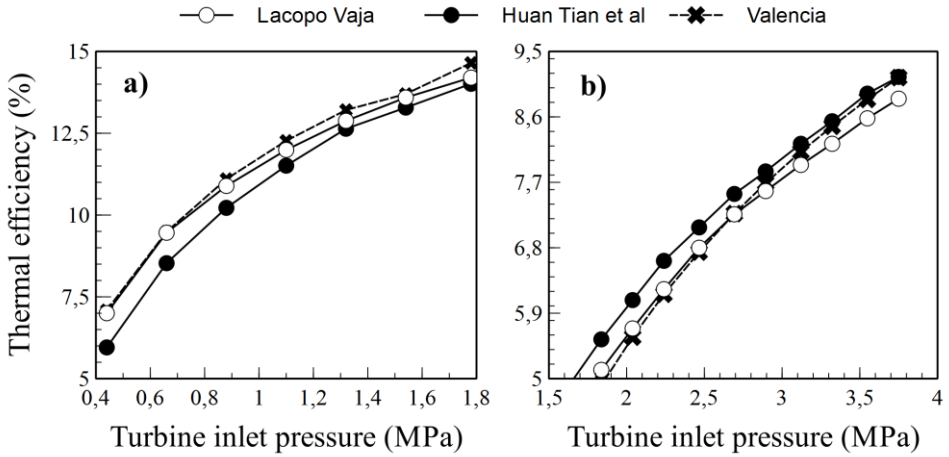

Figure 3. Thermal efficiency of the ORC as a function of the turbine inlet pressure for a) Refrigerant R-11, b) Refrigerant R-134a

The model proposed in this research evinces highly accurate proximity to the results obtained for the same configuration proposed by Lacopo [15] and Huan Tian et al. [18]. In the range evaluated when comparing with the results of Lacopo [15], the error does not exceed 3% for R-11, while for R-134a it presents a maximum error of 6% for turbine inlet pressures less than 1 MPa, moreover, for values greater than 2 MPa the error remains within the range of 3%. Furthermore, the proposed SORC model, evaluated within the pressure range (2.5 MPa - 3 MPa), which is the operating range of the current research, it can be observed that this relative error is under 1% with respect to that proposed by Huan Tian et al. [18], which guarantees the validity of the model, hence the accuracy of the results.

In the case of the validation of the configuration model for a RORC, the results of this system for a geothermal application were taken as references [38], [20]. The parameters considered for both investigations are shown in

Table **7**.

Table 7. Data used from the system for model validation.

η_B	η_T	T_{fuente} [ºC]	F [kg/s]	T_{Cond} [ºC]	Pinch Point [ºC]	P_{Vap} [Mpa]
0,95	0,89	165	84,36.	15	10	0,31

Several considerations were assumed to perform the comparative analysis of the RORC, such as, the processes and subsystems were assumed in steady state, all devices were considered in adiabatic conditions, the pressure drops in the ORC devices and in the pipes are neglected, in dead state the reference temperature was 288 K. The comparison of the simulation results obtained in the model proposed in this research with the results available in the literature are shown as in Table 8. As observed for the three thermodynamic models, it exists a proper fit between the values of the parameters calculated in this work and those previously published [38], [20]. Consequently, in the case of isobutane as an organic working fluid, a percentage error between 0,73% and 0,62% for thermal efficiency was obtained when compared with the work of R. S. El-Emam et al. and V. Zare respectively. In the other hand, exergy efficiency percentage errors obtained were 0,18% and 0,35% respectively, which allows this model to be used for the evaluation of this configuration operating as a heat recovery system.

Table 8. Validation of the proposed model for RORC

Parameters	**Proposed Model**	**R. S. El-Emam et al.** [38]	**V. Zare [20]**
$T_{1\,AT}\ (°C)$	165	165	165
$\dot{m}_{1\,AT}\ (kg/s)$	84,36	84,36	82,16
$\dot{m}_{1\,ORC}\ (kg/s)$	75,22	78,06	76,09
$A_{ITC\,2}\ (m^2)$	394,21	399,30	390,60
$A_{ITC\,3}\ (m^2)$	809,52	810,10	808,70
$A_{RC}\ (m^2)$	124,58	124,80	124,20
$\eta_{th}\ (\%)$	16,25	16,37	16,15
$\eta_{exe}\ (\%)$	48,71	48,80	48,54

4. Results and discussions

From the simulation results obtained, it is possible to determine and calculate the properties of the main streams for the heat recovery system with single ORC, RORC, and DORC, the results are shown in Appendix B Table **B.14** B.1 for the case of SORC.

For each component of the system were applied mass and energy balances, the main results obtained for the heat recovery system assembled with the engine are shown in

Table **9** respectively.

Preprints (www.preprints.org) | NOT PEER-REVIEWED | Posted: 20 May 2019 doi:10.20944/preprints201905.0247.v1

Peer-reviewed version available at Energies 2019, 12, 2378; doi:10.3390/en12122378

Table 9. Parameters of an integrated recovery system with engine and ORC

Parameters	SORC	RORC	DORC.	Units
Thermal efficiency engine-ORC	40,45	41,25	40,72	%
Increased thermal efficiency	1,86	2,66	2,13	%
Thermal efficiency ORC	16,40	23,51	18,74	%
Global energy conversion efficiency	6,68	9,59	7,66	%
Global exergetic efficiency	34,5	49,47	39,43	%
BSFC engine-ORC	169,5	166,21	168,42	g/kWh

An exergy balance was applied to each of the components of the system in order to calculate the exergy for every stream, which results are presents as in Table 10 through the Input-Output definition in every component of the SORC configuration.

Table 10. Exergy values for each component of the heat recovery system with SORC

Component	Input (kW)	Product (kW)	$\dot{E}x_D$(kW)	Lost (kW)
ITC1	541,202051	202,794262	41,9535673	296,454222
B1	0,37472727	0,05848531	0,31624196	
ITC2	202,852748	166,340104	36,5126437	
T1	99,4808146	85,5899807	13,8908338	
ITC3			36,0581887	66,5877282
B2	0,75619324	0,58683347	0,16935977	

The fraction of exergy destroyed in each component of the cycle was calculated from the results of the Input-output definition; the exergy destruction percentages are presented as in Figure 4a.

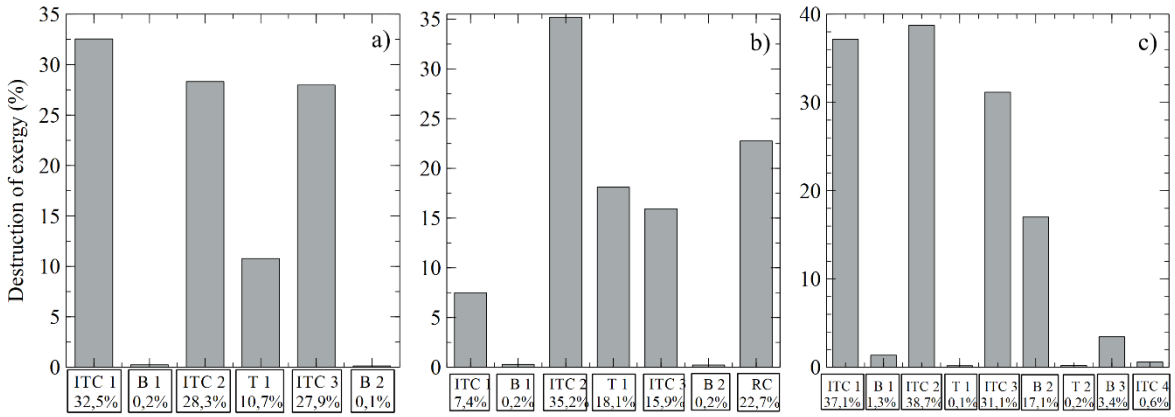

Figure 4. Exergy destruction by heat recovery system component a) SORC, b) RORC and c) DORC

It is observed that a large part of the exergy is destroyed in the tube and shell heat exchanger (ITC1) with a value of 32,5%, followed by the evaporator with 28,3%, and condenser with 27,9%, while the pumps in system present the lowest fractions of exergy destruction. Due to operational restrictions on the temperature at the organic fluid to the turbine inlet, it is not possible to lower the minimum temperature in the evaporator in order to obtain less entropy generated and thus less

exergy destroyed in this equipment. Nevertheless, these temperature differences in heat exchangers must be optimized for better performance.

The use of isentropic and dry fluids in the RORC, allows obtaining relatively high temperatures of the organic fluid at the exit of the turbine (2ORC stream) with superheated steam state [39], as is the case of Toluene for this process as shown in Appendix B

Table B.**2**. Therefore, the internal heat exchanger (RC) absorbs the heat from the working fluid leaving the turbine (T1) and increase the temperature of the fluid entering the evaporator (6ORC stream) [40].

The heat transfers from the fluid at the turbine outlet to the fluid at the evaporator inlet that occurs in the recuperator [41], allows an absolute increase the thermal efficiency of 2,6%, while in SORC the increase presented was 1,8%. Consequently, the overall configuration presents a specific fuel consumption of 166,21 g/kWh, 2% less than the SORC configuration as shown in

Table 9 for the same operating conditions with Toluene.

The efficiency and performance indicators of this configuration increase with the inclusion of heat recovery system, due to it is possible, for an equal amount of heat entering the cycle, through ITC1, to increase the power generation in the turbine. The improvement in efficiency varies according to the working fluid and is directly related to its properties, primarily its specific heat [42]. The results confirm that the recovery system has no effect on the power of the turbine and pump, however, it directly influences the heat transfer in the evaporator and condenser [43], equipment where are the highest irreversibility as shown in Table 11, obtaining exergy destruction values 33,82 kW (35,2%) in the evaporator, followed by the recuperator with 21,86 kW (22,8%).

Table 11. Exergy values for each component of the heat recovery system with RORC

Component	Input (kW)	Product (kW)	$\dot{E}x_D$(kW)	Lost (kW)
ITC1	541,202051	237,549898	7,197931	296,454222
B1	0,36222219	0,09598314	0,26623905	
ITC2	237,645881	203,818309	33,827572	
T1	139,797975	122,396844	17,40113113	
ITC3			15,3197	71,5691491
B2	0,94533621	0,7336153	0,21172091	
RC	86,4902041	64,620999	21,8692051	

Furthermore, the fraction of exergy destroyed in each component of the cycle is presented in Figure 4b, where the percentage contribution of the pumps only reaches 0.5% of the total exergy destruction of the system.

For the DORC configuration there are two different evaporating pressures, however the 2 ORC, 2′ ORC and 2″ ORC streams are mixed at the same pressure to perform work in the Turbine (T1). Moreover, at the outlet of the low-pressure pump (B2) the states 5 ORC, 5′ ORC and 5″ ORC have similar thermodynamic properties with different mass flows as shown in Appendix B in Table B.3.

Table **9** presents the performance parameters of the integrated system with ICE and DORC, where it is observed that this configuration in the evaluated conditions only achieves an overall energy conversion efficiency of 6,68% and an overall exergetic efficiency of 34,37%. These results are directly related to the pressure ratio values selected for this base case, according to state of the art, this configuration presents a better exergy efficiency, and permits generating more power than the SORC configuration and RORC [44].

In this configuration, the high-pressure evaporator (ITC 4) along together with the tube and shell heat exchanger (ITC1) are the equipment where the highest exergy destruction levels are presented as in Table 12 due to the temperature differences between the thermal oil and the organic fluid.

Table 12. Exergy values for each component of the heat recovery system with DORC

Component	Input (kW)	Product (kW)	$\dot{E}x_D$(kW)	Lost (kW)
ITC1	541,20	203,57	31,15	296,45
B1	1,66	0,26	1,40	
ITC2	113,18	101,93	11,26	
T1	95,39	79,75	15,63	
ITC3			31,01	6,00
B2	0,63	0,49	0,14	
T2	10,27	8,77	1,49	
B3	2,09	1,63	0,47	
ITC4	90,64	52,66	37,99	

The fraction of exergy destruction per component for the dual ORC heat recovery system is shown as in Figure 4c, where evaporators and condensers contribute about 86,4% of the total destroyed exergy. As the organic fluid evaporates in the heat exchangers at proper evaporating pressure, a closer match can be maintained between the thermal oil cooling curve in the secondary coupling circuit and the heating or boiling curve of the working fluid, consequently these losses can be reduced.

4.1. Sensitivity analysis

4.1.1 Analysis of the influence of the evaporation pressure on the performance of the configurations.

Considering the relevance of the evaporation pressure on the operation of these systems, a comparative analysis of the net power, an absolute increase of thermal efficiency and absolute decrease of the specific consumption of fuel for the SORC, RORC, and DORC is presented in Figure 5. For the dual cycle, the values of high evaporation pressure were reached by varying the pressure ratio of the B3 pump, with the pressure ratio values of the B2 pump fixed at 3 for Toluene, 10 for Acetone and 1,5 for Cyclohexane.

It is observed that the power generated is directly related to the evaporation pressure, obtaining for the evaluated conditions the most profitable results for the cycle with recovery efficiency of 80% in the recuperator, operating with Toluene at an evaporation pressure of 3,4 MPa, with a maximum power of 146,25 kW, which is equivalent to 31,9% more than the energy generated with the same fluid as in the SORC at the same pressure. While varying the pressure ratio of the B3 pump in a dual cycle is not possible to achieve the same evaporating pressure as the fluid is heated to the point of reversing heat transfer in the evaporator with the thermal oil.

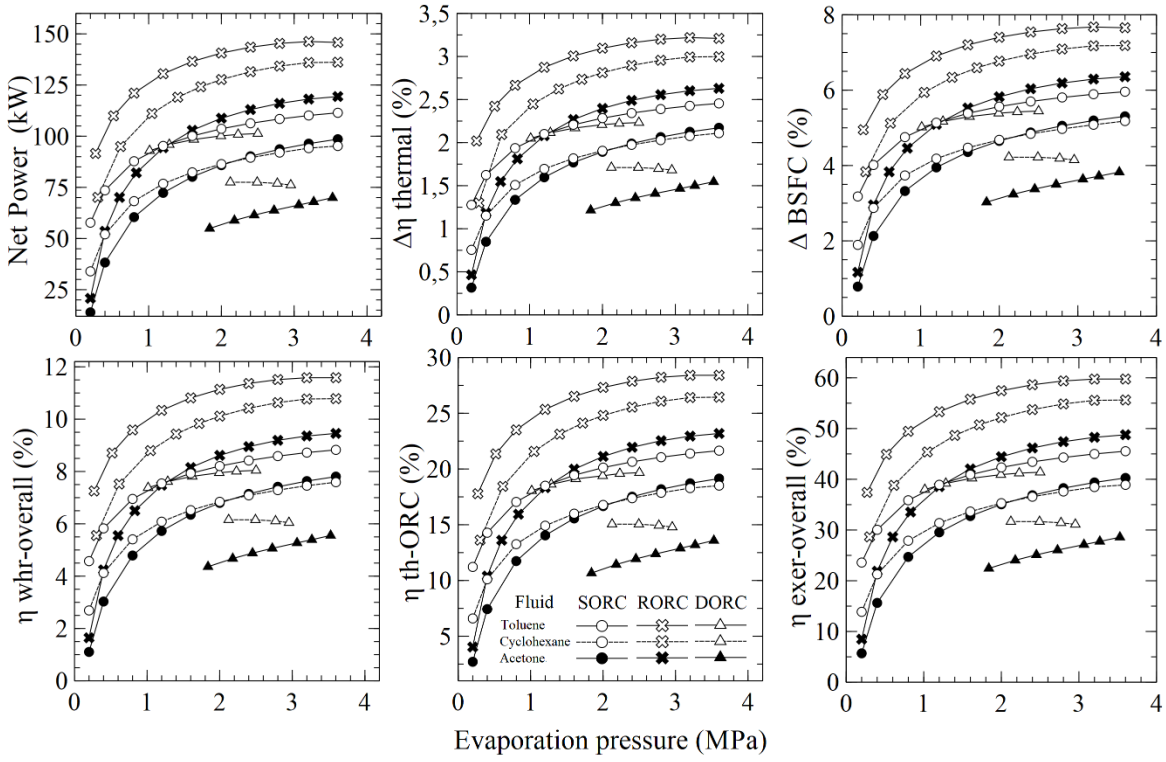

Figure 5. Performance of SORC, RORC and DORC configurations with different organic fluids, a) Net power, b) Absolute increase in thermal efficiency, c) Absolute decrease in specific fuel consumption, d) Global energy conversion efficiency, e) ORC thermal efficiency and f) Global exergetic efficiency.

When comparing the absolute increase in thermal efficiency for the three ORC configurations proposed in Figure 5b, it can be observed that the influence of the evaporating pressure is to increase the efficiency to an upper limit [45], [46]. In the case of Toluene, at the same evaporation pressure of 3,4 MPa, the simple ORC increases the efficiency of the generation engine by 2,44%, while the regeneration cycle increases by 3,22%. Working fluids such as acetone and cyclohexane in the simple cycle achieve an absolute increase in the thermal efficiency of 2,15% and 2,09% respectively; henceforth Toluene is the working fluid that in addition to meet the requirements of fluid selection design, presents the best results operating in simulation. Furthermore, due to the main objective of this research is to increase the thermal efficiency of the cycle and the generation of additional power, a recovery system is the best option regardless of the working fluid. Which is confirmed by the results of Figure 5, where the most profitable values of specific fuel consumption decrease a 5,92% and 7,67% working with Toluene in the simple configuration and heat recovery respectively, while the lowest value in the evaluated range was presented working with Acetone with the simple cycle with a value of 0,78% at an evaporation pressure of 0,2 MPa. However, there are several disadvantages of the RORC, as the heat in the evaporator increases, the heat exchanger would have the highest acquisition costs from the proposed configurations.

Through evaluating the overall energy conversion efficiency as shown in Figure 5d, Toluene and Cyclohexane have values of 8,78% and 7,54% with the SORC cycle configuration in the base operating condition of the ICE and evaporating pressure of 3,4 MPa. For the configuration RORC, the lowest yields at the same pressure were presented for Acetone, with a value of 9,41%, which confirms that Toluene is the potential fluid to be used in the process as in the SORC and RORC.

The highest value for thermal efficiency of the ORC and global exergetic efficiency obtained were obtained for the RORC, where the assembly of the recovery system to the evaporation pressure of 3,4 MPa, for the Toluene, increased the thermal efficiency from 21,53% to 28,41% and the global exergetic efficiency from 45,29% to 59,76%, which confirms the excellent performance of Toluene at relatively low pressures. The maximum power generated by the SORC configuration working with Toluene seize approximately 8,31% of the generating capacity of the Jenbacher JMS 612 GS-N. L engine at rated load speed. Additionally, it is observed that toluene in a SORC, increasing the evaporation pressure from 2 MPa to 3 MPa, leads to a 5,49% increase in the power generated within a range from 103,61 kW to 109,3 kW. The absolute increase in thermal efficiency varies approximately 5,26% within values from 2,28% to 2,40%. Finally, the absolute decrease in specific fuel consumption is higher by 5,21% given the increase presented from 5,56% to 5,85% respectively. On the other hand, in the case of the cycle with recovery, the percentage increases for these variables were 3,76%, 3,75% and 3,47%, which allows us to conclude that this variable is more influential in the SORC configuration.

4.4.2 Analysis of the influence of evaporation pressure on the destruction of exergy configurations

In order to perform a comparative analysis of the exergetic performance for each ORC configuration, the fractions of exergy destruction in each component of the cycle were calculated with the three proposed working fluids. The exergy destruction fractions for each ORC configuration are shown as in Figure 6, at different evaporating pressures for Acetone, Cyclohexane, and Toluene.

The results demonstrate that the exergy fractions for the DORC cycle are higher than the SORC, while the RORC cycle has the lowest values of total exergy loss.

Preprints (www.preprints.org) | NOT PEER-REVIEWED | Posted: 20 May 2019 doi:10.20944/preprints201905.0247.v1

Peer-reviewed version available at Energies 2019, 12, 2378; doi:10.3390/en12122378

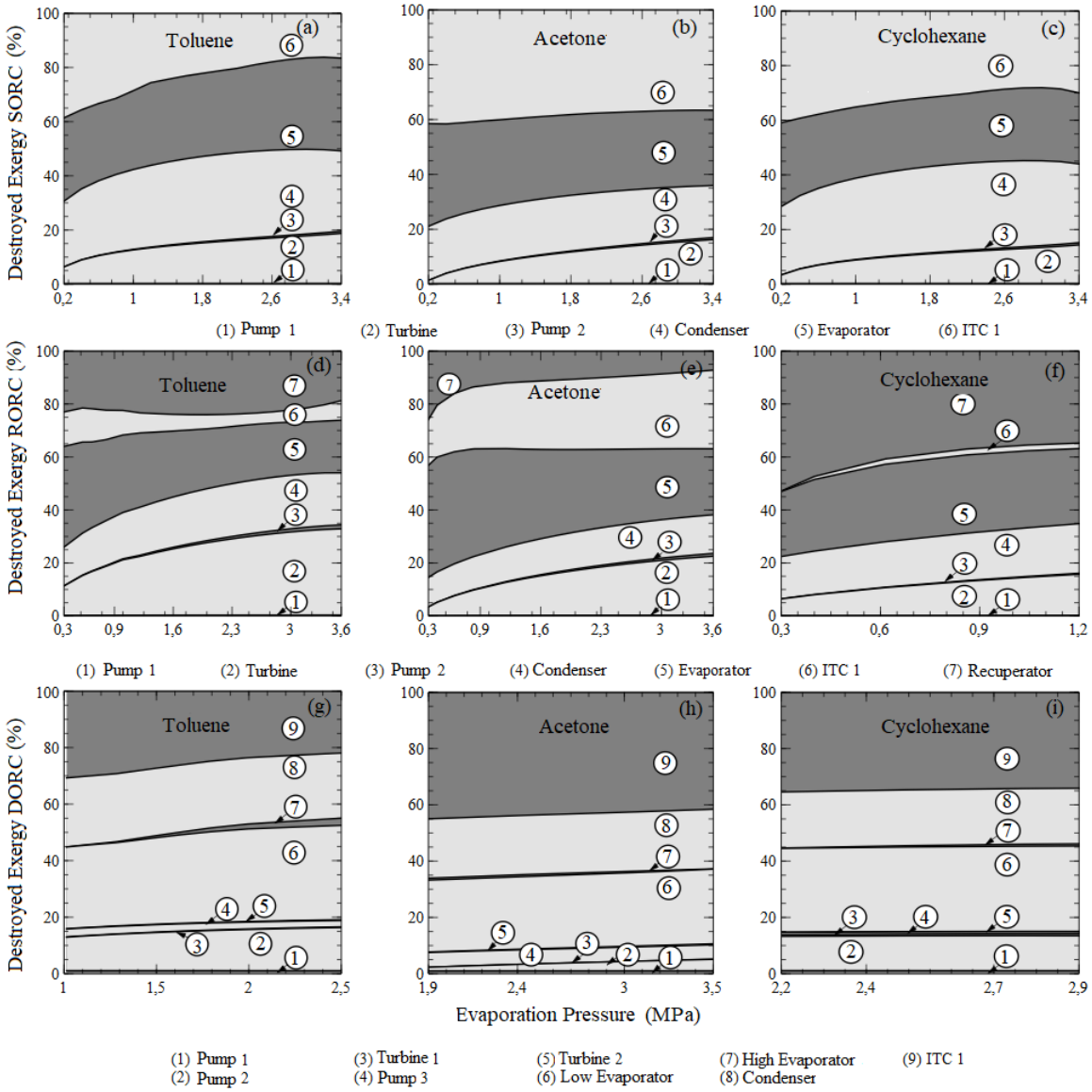

Figure 6. exergy destruction by component as a function of evaporating pressure for (**a**, **b** and **c**) configuration SORC, (**d**, **e** and **f**) configuration RORC and (**g**, **h** and **i**) configuration DORC

After the evaluation of the average decrease in percentage points of the three configurations studied to the engine operating condition, it was demonstrated that the DORC cycle, working with Toluene presents an average of 74,02% total exergy destruction, more significant than the exergy destruction in RORC configuration. These results are due to the DORC configurations lead to higher exergy destruction by having more components. However, in an operational range of evaporating pressure, the dual ORC exceeds the destroyed exergy of the SORC by 9%. Consequently, the evaporating pressure must be determined for each specific case to achieve the highest turbine output power, and thus greater exergetic efficiency of the system.

The DORC configuration presents the highest values of exergy destruction fractions operating with Acetone within the temperature range of the source studied, while the SORC configuration presents the lowest values of exergy destruction fraction. As a result, the SORC configuration delivers more power to the least heat rejection in the condenser; additionally, for the same power delivered, this configuration requires less heat from the heat source. The results also show that the evaporating

pressure in the different ORC configurations has a significant effect on the total dimensionless exergy losses, with a minimum value within the range studied.

The maximum values of exergy losses occurred in the condenser for every configuration, with a maximum value of 88,26% for the SORC at 0,803 MPa. As a result, the exergy destruction fractions in the condenser is inversely proportional to the evaporating pressure as it approaches 2 MPa. Due to the significant increase in exergy losses, the evaporator and turbine cycle, in the RORC, the recuperator acquires importance, while in the dual cycle the low evaporator provides exergy destruction as the pressure increases.

4.1.3 Analysis of the influence of engine load on energy performance

This section analyzes the effect of engine load on the performance of the heat recovery system. The results presented above were obtained based on the typical operating condition of a natural gas engine. The engine power control system adjusts internal engine variables such as mixture pressure, and temperature and mixture recirculation percentage to provide high efficiency in operations with partial engine loads. The global energy indicators were selected as study variables, and the results of the three configurations under study for an evaporating pressure of 675,8 kPa working with Toluene, are shown as in Figure 7. For safety reasons, all possible operating points of the proposed configurations at different engine loads, guarantee that Toluene vaporizes completely at the evaporator outlet in order to prevent corrosion of the liquid in the expander. Moreover, the engine exhaust gas temperature at the evaporator outlet (stream 11) must be higher than the acid spray temperature (200 °C) to prevent acid corrosion of the exhaust.

The thermal efficiency presents a directly proportional relationship with respect to the engine load increases, while the overall energy conversion efficiency presents an inversely proportional relationship. The maximum net output power obtained for configurations at engine load percentages is SORC (89,4 kW – 97,9%), RORC (124,5 kW – 97,9%) and DORC (86,29 kW – 91,81%). However, in an engine operating interval, the thermal efficiency increase as the RORC configuration increases first and then decreases, presenting a maximum performance with 82,68% engine load.

These results are due to the engine load is directly related to the flow in the exhaust gases and the energy loss in the recuperator, since the evaporation pressure and the temperatures of the thermal coupling oil have been restricted. As the operating load increases, there is an increase in the evaporation temperature of the organic fluid. Therefore, the power increases, which is the main factor that affects the thermal and exergetic efficiency. However, the isentropic efficiency of the turbine decreases slightly as a consequence of the increase in the temperature of the thermal oil, causing a decrease in the indicators at high engine loads. The direct relation between the net power and the engine load is also due to the increase of the thermal oil inlet temperature to the evaporator, which leads to an increase in the mass flow of Toluene, and the enthalpy difference between the pump and the turbine, however, this causes a stronger effect in the turbine.

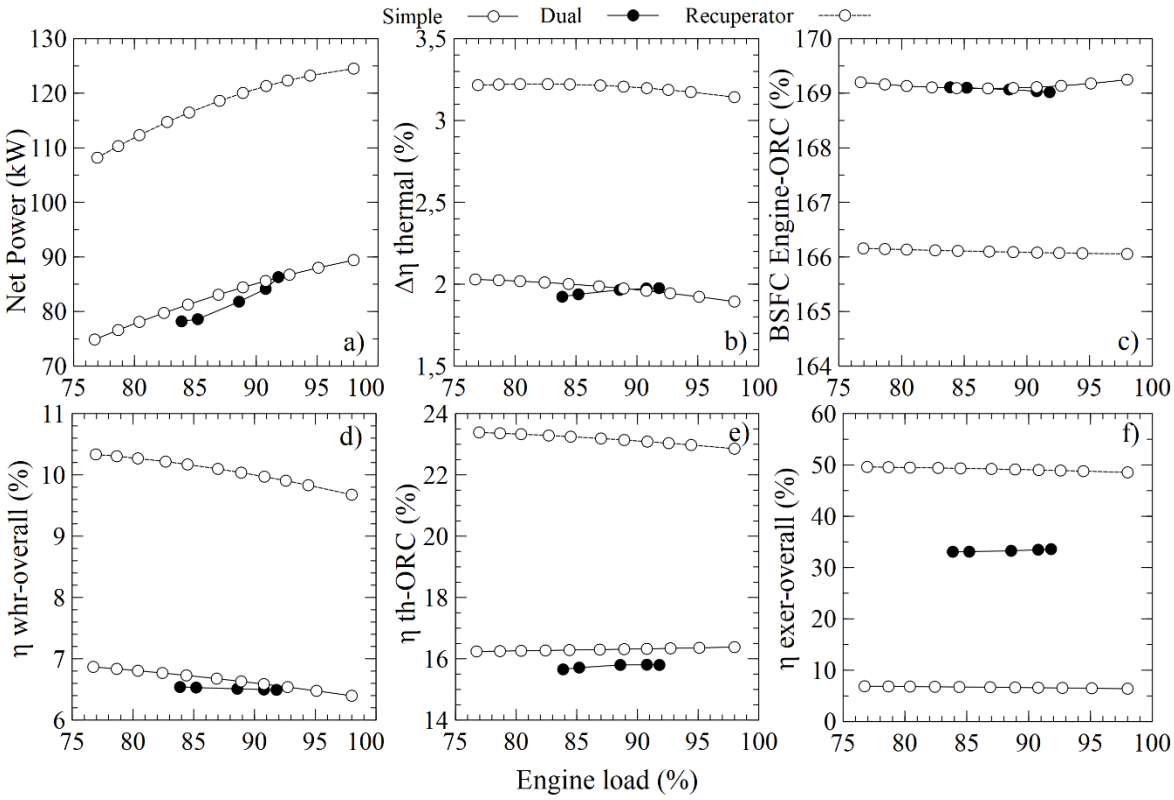

Figure 7. Performance of SORC, RORC and DORC configurations with different engine loads, a) Net power, b) Absolute increase in thermal efficiency, c) Specific fuel consumption of engine - ORC, d) Overall energy conversion efficiency, e) ORC thermal efficiency and f) Overall exergetic efficiency.

5. Conclusions

The study allowed an energetic and exergetic analysis of three energy generation systems based on ORC, to waste heat recovery from the exhaust gases of a generation engine using natural gas as fuel in a plastic industry located in the Colombian Caribbean region. In particular, the results obtained through a dynamic model validated with experimental data is used to know the exhaust gases temperature, power output, fuel consumption and thermal efficiency of the gas engine based on the mean variables of the system. The study involved the thermodynamic model development and the research of energy and exergy performance indicator of the integrated engine system with three configurations of waste heat recovery, to determine the improvement degree of the thermal efficiency of the Jenbacher JMS 612 GS-N. L of 2 MW.

To propose a thermal system with a better performance, the irreversibilities and exergy destruction of the components must be reduced. The destroyed exergy of all the elements in the different configurations is low compared to the thermal oil pump (B1). These values suggest that reducing the heat transfer area in the evaporator, recuperator, and condenser may provide a favorable solution, especially in the DORC configuration. However, it is essential to note that these plate heat exchangers are manufactured from specialized materials for these applications, which contributes significantly to the total purchase cost of the systems. Also, the operation of this equipment has a significant effect on the total exergy destruction and thermal efficiency of the system as a result of the Pinch Point temperature. Therefore, increasing the size of heat exchangers increases the cost of generating electricity.

The thermal oil pump is the equipment with the lowest efficiency from all the system components, SORC (16%), RORC (26%) and DORC (17%). However, among the heat exchange equipment, the shell and tube heat exchanger (ITC1) has the lowest exergetic efficiency in the three configurations SORC (37%), RORC (44%) and DORC (38%), due to the organic fluid cannot reach the engine exhaust gas temperature levels due to the increase of heat transfer irreversibilities and thermal stability conditions. Hence, these alternatives present better results with medium and low quality thermal sources of Exhaust gases.

The exergy destruction in ITC1 is the most important for the SORC and DORC applications, while the evaporator (ITC2) is the most important for the RORC. Therefore, the effort should be oriented to reducing the exergy destruction in these components. Based on commercial information on the geometric characteristics of the plate heat exchangers and shell and tube heat exchanger, the optimal sizes of these types of equipment for the different configurations should be determined.

Author Contributions: Conceptualization: G.V.; Methodology: G.V. and F.C.; Software: G.V., F.C. and Y.C.; Validation: G.V., F.C. and Y.C.; Formal Analysis: G.V., J.D. and C.I.; Investigation: G.V.; Resources: Y.C. and F.C.; Writing-Original Draft Preparation: G.V.; Writing-Review & Editing: J.D. and C.I.; Funding Acquisition: G.V.

Funding: This work was supported by the Universidad del Atlántico, Universidad Pontificia Bolivariana and the E2 Energía Eficiente S.A E.S. P company.

Conflicts of Interest: The authors declare no conflict of interest.

Abbreviations

The following abbreviations are used in this manuscript:

BSFC	Brake Specific Fuel Consumption
DORC	Double pressure Organic Rankine Cycle
GHG	Green House Gases
GWP	Global Warming Potential
ICE	Internal Combustion Engine
ORC	Organic Rankine Cycle
RORC	Recuperator Organic Rankine Cycle
SORC	Simple Organic Rankine Cycle
WHR	Waste Heat Recovery

Nomenclature

C_p	Specific heat at constant pressure (J/kg K)
E	Energy (J)
ex	Specific exergy (kJ/kg)
h	Specific enthalpy (kJ/kg)
LHV	Heating power (kj/kg)
m	Mass (kg)
Q	Heat (J)
R	Universal gas constant (atm L/mol K)
rpm	Engine speed (revolution per minutes)
T	Temperature (K)
t	Time (s)
$\dot{W}$	Power (kW)
X_i	Molar gas fraction

Greek Letters

$\eta_{I,c}$	Thermal efficiency of the cycle
$\eta_{I,global}$	Overall energy conversion efficiency
$\eta_{II,ORC}$	Exergetic efficiency
ε_{hr}	Heat recovery efficiency

Preprints (www.preprints.org) | NOT PEER-REVIEWED | Posted: 20 May 2019 doi:10.20944/preprints201905.0247.v1

Peer-reviewed version available at Energies 2019, 12, 2378; doi:10.3390/en12122378

Subscripts

D	Destroyed
G	Gases
VC	Control volume

Appendix A

The energy balance applied to each component of the proposed configurations is presented in Table A.1.

Table A.13. Energy balances for the components of each configuration

Component	Different configurations of residual heat recovery systems using ORC		
	SORC	RORC	DORC
Heat Exchanger 1 (ITC1)	$\dot{Q}_G = \dot{m}_{10} C_{P10}(T_{10} - T_{11}) = \dot{m}_{AT} C_{PAT}(T_{4AT} - T_{3AT})$ (A.1)	(A.1)	(A.1)
Pump 1 (B1)	$\eta_{B1} = \frac{\upsilon_{2AT}(P_{3AT} - P_{2AT})}{h_{3AT} - h_{2AT}}$ (A.2) $\dot{W}_{B1} = \dot{m}_{AT}(h_{3AT} - h_{2AT})$ (A.3)	(A.2)	(A.2)
Heat Exchanger (ITC2)	Zone 1 (Preheating) $\dot{Q}_{Z1} = \dot{m}_{AT}(h_{ATf} - h_{2AT}) = \dot{m}_{ORC}(h_{4fORC} - h_{4ORC})$ (A.4) Zone 2 (Evaporation) $\dot{Q}_{Z2} = \dot{m}_{AT}(h_{ATg} - h_{ATf}) = \dot{m}_{Z2}(h_{fgORC})$ (A.5) Zone 3 (Overheating) $\dot{Q}_{Z3} = \dot{m}_{AT}(h_{1AT} - h_{ATg}) = \dot{m}_{ORC}(h_{1ORC} - h_{4gORC})$ (A.6)	$\dot{Q}_{Z1} = \dot{m}_{AT}(h_{ATf} - h_{2AT}) = \dot{m}_{ORC}(h_{6fORC} - h_{6ORC})$ (A.13) Zone 2 (A.5) $\dot{Q}_{Z3} = \dot{m}_{AT}(h_{1AT} - h_{ATg}) = \dot{m}_{ORC}(h_{1ORC} - h_{4gORC})$ (A.14)	$\dot{Q}_{Z1} = \dot{m}_{AT}(h_{ATf} - h_{2AT}) = \dot{m}_{ORC}(h_{5fORC} - h_{5ORC})$ (A.21) Zone 2 (A.5) $\dot{Q}_{Z3} = \dot{m}_{AT}(h_{1-2AT} - h_{ATg}) = \dot{m}_{5ORC}(h_{2ORC} - h_{5gORC})$ (A.22)
Turbine 1 (T1)	$\eta_{T1} = \frac{h_{1ORC} - h_{2ORC}}{h_{1ORC} - h_{2SORC}}$ (A.7) $\dot{W}_{T1} = \dot{m}_{ORC}(h_{1ORC} - h_{2ORC})$ (A.8)	(4A.7) (4A.8)	$\eta_{T1} = \frac{h_{2''ORC} - h_{3ORC}}{h_{2''ORC} - h_{3SORC}}$ (A.29) $\dot{W}_{T1} = (\dot{m}_{5ORC} + \dot{m}_{6ORC})(h_{2''ORC} - h_{3ORC})$ (A.30)

Heat Exchanger (ITC3)	Cooling $\dot{Q}_{ZE} = \dot{m}_{ORC}(h_{2ORC} - h_{2gORC}) = \dot{m}_{1A}(h_{2A} - h_{1gA})$ (A.9) Condenser $\dot{Q}_{ZC} = \dot{m}_{ZC}(h_{2gORC} - h_{3ORC}) = \dot{m}_{1A}(h_{1gA} - h_{1A})$ (A.10)	$\dot{Q}_{ZE} = \dot{m}_{ORC}(h_{3ORC} - h_{3gORC}) = \dot{m}_{1A}(h_{2A} - h_{1gA})$ (A.15) $\dot{Q}_{ZC} = \dot{m}_{ZC}(h_{3gORC} - h_{4ORC}) = \dot{m}_{1A}(h_{1gA} - h_{1A})$ (A.16)	(A.15) (A.16)
Pump 2 (B2)	$\eta_{B2} = \frac{v_{3ORC}(P_{4ORC} - P_{3ORC})}{h_{4ORC} - h_{3ORC}}$ (A.11) $\dot{W}_{B2} = \dot{m}_{ORC}(h_{4ORC} - h_{3ORC})$ (A.12)	$\eta_{B2} = \frac{v_{4ORC}(P_{5ORC} - P_{4ORC})}{h_{5ORC} - h_{4ORC}}$ $\dot{W}_{B2} = \dot{m}_{ORC}(h_{5ORC} - h_{4ORC})$ (A.18)	$\eta_{B2} = \frac{v_{4ORC}(P_{5ORC} - P_{4ORC})}{h_{5ORC} - h_{4ORC}}$ (A.27) $\dot{W}_{B2} = (\dot{m}_{5ORC} + \dot{m}_{6ORC})(h_{5ORC} - h_{4ORC})$ (A.28)
RC	-	$\varepsilon_{RC} = \frac{T_{2ORC} - T_{3ORC}}{T_{2ORC} - T_{5ORC}}$ (A.19) $\dot{Q}_{RC} = \dot{m}_{ORC}(h_{6ORC} - h_{5ORC}) = \dot{m}_{ORC}(h_{2ORC} - h_{3ORC})$ (A.20)	-
Turbine 2 (T2)	-	-	$\eta_{T2} = \frac{h_{1ORC} - h_{2,ORC}}{h_{1ORC} - h_{2,SORC}}$ (A.25) $\dot{W}_{T2} = \dot{m}_{6ORC}(h_{1ORC} - h_{2,ORC})$ (A.26)
Pump 3 (B3)	-	-	$\eta_{B3} = \frac{v_{5ORC}(P_{6ORC} - P_{5ORC})}{h_{6ORC} - h_{5ORC}}$ (A.31) $\dot{W}_{B3} = \dot{m}_{6ORC}(h_{6ORC} - h_{5ORC})$ (A.32)

Heat Exchanger (ITC4)	-	-	$\dot{Q}_{Z1} = \dot{m}_{AT}(h_{ATf} - h_{1-2AT}) = \dot{m}_{6ORC}(h_{6fORC} - h_{6ORC})$ (A.23) Zone 2 (A.5) $\dot{Q}_{Z3} = \dot{m}_{AT}(h_{1AT} - h_{1-ATg}) = \dot{m}_{6ORC}(h_{1ORC} - h_{6gORC})$ (A.24)

Appendix B

The properties of the main currents of the heat recovery system proposed with SORC are presented in Table B.14.

Table B.14. Properties considered for SORC configuration

Stream	Flow (kg/s)	P. (kPa)	T. (°C)	Enthalpy (kJ/kg)	Entropy(S-S0) (kJ/kg K)	Exergy (kW)
10	2,77	102,30	435,07	-1960,35	0,90	541,20
11	2,77	101,30	270,00	-2143,67	0,59	296,45
1 AT	1,64	101,43	307,84	461,66	0,94	208,75
1 ATg	1,64	91,42	246,29	324,52	0,73	106,76
1 ATf	1,64	81,01	178,30	183,24	0,47	29,12
2 AT	1,64	68,15	142,65	113,96	0,31	5,90
3 AT	1,64	170,38	142,77	114,19	0,31	5,96
1 ORC	0,72	675,85	272,84	633,29	1,80	169,27
2 ORC	0,72	22,53	202,37	513,72	1,87	69,79
2 gORC	0,72	22,53	65,00	301,64	1,34	31,18
3 ORC	0,72	22,53	65,00	-87,53	0,19	2,35
4 ORC	0,72	675,85	65,31	-86,47	0,19	2,93
4 fORC	0,72	675,85	194,20	181,72	0,86	50,17
4 gORC	0,72	675,85	194,20	477,95	1,50	124,68
1 A	13,32	101,30	50,00	209,42	0,27	35,20
1 gA	13,32	101,30	55,00	230,33	0,33	54,44
2 A	13,32	101,30	57,72	241,72	0,37	66,59

The properties of the main currents of the heat recovery system proposed with RORC are presented in

Table B.**2**.

Table B.2. Properties considered for RORC configuration

Stream	Flow (kg/s)	P. (kPa)	T. (°C)	Enthalpy (kJ/kg)	Entropy(S-S0) (kJ/kg K)	Exergy (kW)
10	2,77	102,30	435,07	-1960,35	0,90	541,20
11	2,77	101,30	270,00	-2143,67	0,59	296,45
1AT	1,51	101,43	374,47	618,96	1,25	263,92
1ATg	1,51	92,78	379,55	631,30	1,27	273,93
1ATf	1,51	83,89	294,56	431,40	0,98	126,19
2AT	1,51	68,15	209,28	246,22	0,65	26,27
3AT	1,51	170,38	209,40	246,46	0,65	26,37
1ORC	0,89	675,85	339,47	775,16	2,05	272,11
2ORC	0,89	22,53	268,70	638,39	2,11	132,31
3ORC	0,89	22,53	102,23	352,50	1,49	45,82
3gORC	0,89	22,53	65,00	301,64	1,34	38,98
4ORC	0,89	22,53	65,00	-87,53	0,19	2,93
5ORC	0,89	675,85	65,31	-86,47	0,19	3,67
6ORC	0,89	675,85	194,20	199,42	0,90	68,29
6fORC	0,89	675,85	194,20	181,72	0,86	62,72
6gORC	0,89	675,85	194,20	477,95	1,50	155,86
1A	16,65	101,30	50,00	209,42	0,27	44,00
1gA	16,65	101,30	55,00	230,33	0,33	68,06
2A	16,65	101,30	55,65	233,06	0,34	71,57

The properties of the main currents of the heat recovery system proposed with DORC are presented in Table B.3.

Table B.3. Properties considered for DORC configuration

Stream	Flow (kg/s)	T. (°C)	P. (kPa)	Enthalpy (kJ/kg)	Entropy (S-S0) (kJ/kg K)	Exergy (kW)
10	2,77	435,07	102,30	-1960,35	0,90	541,20
11	2,77	270,00	101,30	-2143,67	0,59	296,45
1 AT	1,62	316,58	686,83	481,81	0,99	215,40
1 ATg	1,62	296,48	676,43	435,75	0,92	178,88
1 ATf	1,62	245,76	666,37	323,37	0,74	99,29
1-2 AT	1,62	171,41	656,79	169,58	0,44	20,13
1-2 ATg	1,62	228,96	647,85	287,41	0,68	77,18
1-2 Atf	1,62	183,04	638,85	192,71	0,49	29,19
2 AT	1,62	150,98	630,14	129,89	0,35	7,53
3AT	1,62	151,51	755,78	130,91	0,35	7,80
1A	8,40	50,00	101,30	209,42	0,27	27,60
1g A	8,40	55,00	101,30	230,33	0,33	42,69
2A	8,40	55,00	101,30	234,54	0,34	46,10
1 ORC	0,45	281,58	1351,69	635,64	1,75	159,64

2 ORC	0,62	136,41	450,56	53,17	0,57	13,75
2′ ORC	0,45	252,65	450,56	597,65	1,77	132,33
2″ ORC	1,08	173,03	450,56	368,93	1,28	139,83
3 ORC	1,08	65,00	22,53	298,79	1,34	46,85
3g ORC	1,08	65,00	22,53	301,64	1,34	47,17
4 ORC	1,08	65,00	22,53	-87,53	0,19	3,55
5 ORC	1,08	65,21	450,56	-86,84	0,19	4,13
5′ ORC	0,45	65,21	450,56	-86,84	0,19	2,40
5″ ORC	0,62	65,21	450,56	-86,84	0,19	1,74
5f ORC	0,62	173,04	450,56	132,93	0,76	24,32
5g ORC	0,62	173,04	450,56	447,79	1,46	70,24
6 ORC	0,45	65,64	1351,69	-85,38	0,20	3,10
6f ORC	0,45	235,75	1351,69	283,87	1,07	68,73
6g ORC	0,45	235,75	1351,69	535,81	1,56	132,70

References

[1] Z. Mat Nawi, S. K. Kamarudin, S. R. Sheikh Abdullah, and S. S. Lam, "The potential of exhaust waste heat recovery (WHR) from marine diesel engines via organic rankine cycle," *Energy*, vol. 166, no. 255, pp. 17–31, 2019.

[2] F. Alshammari, A. Pesyridis, A. Karvountzis-Kontakiotis, B. Franchetti, and Y. Pesmazoglou, "Experimental study of a small scale organic Rankine cycle waste heat recovery system for a heavy-duty diesel engine with focused on the radial inflow turbine expander performance," *Appl. Energy*, vol. 215, no. 122, pp. 543–555, 2018.

[3] P. Liu, G. Shu, H. Tian, X. Wang, and Z. Yu, "Alkanes based two-stage expansion with interheating Organic Rankine cycle for multi-waste heat recovery of truck diesel engine," *Energy*, vol. 147, no. 866, pp. 337–350, 2018.

[4] C. N. Michos, S. Lion, I. Vlaskos, and R. Taccani, "Analysis of the backpressure effect of an Organic Rankine Cycle (ORC) evaporator on the exhaust line of a turbocharged heavy duty diesel power generator for marine applications," *Energy Convers. Manag.*, vol. 132, no. 25, pp. 347–360, 2017.

[5] P. S. Patel and E. F. Doyle, "Compounding the Truck Diesel Engine with an Organic Rankine-Cycle System." SAE International , 1976.

[6] B. Peris, J. Navarro-Esbrí, and F. Molés, "Bottoming organic Rankine cycle configurations to increase Internal Combustion Engines power output from cooling water waste heat recovery," *Appl. Therm. Eng.*, vol. 61, no. 2, pp. 364–371, 2013.

[7] G. Yu, G. Shu, H. Tian, H. Wei, and L. Liu, "Simulation and thermodynamic analysis of a bottoming Organic Rankine Cycle (ORC) of diesel engine (DE)," *Energy*, vol. 51, no. 1–474, pp.

281–290, 2013.

[8] Y. Lu, Y. Wang, C. Dong, L. Wang, and A. P. Roskilly, "Design and assessment on a novel integrated system for power and refrigeration using waste heat from a diesel engine," *Appl. Therm. Eng.*, vol. 91, pp. 591–599, 2015.

[9] R. Chacartegui, D. Sánchez, J. M. Muñoz, and T. Sánchez, "Alternative ORC bottoming cycles FOR combined cycle power plants," *Appl. Energy*, vol. 86, no. 10, pp. 2162–2170, 2009.

[10] K. Qiu and A. C. S. Hayden, "Integrated thermoelectric and organic Rankine cycles for micro-CHP systems," *Appl. Energy*, vol. 97, no. 457–889, pp. 667–672, 2012.

[11] U. Drescher and D. Brüggemann, "Fluid selection for the Organic Rankine Cycle (ORC) in biomass power and heat plants," *Appl. Therm. Eng.*, vol. 27, no. 1, pp. 223–228, 2007.

[12] P. J. Mago, L. M. Chamra, K. Srinivasan, and C. Somayaji, "An examination of regenerative organic Rankine cycles using dry fluids," *Appl. Therm. Eng.*, vol. 28, no. 8, pp. 998–1007, 2008.

[13] G. Kosmadakis, D. Manolakos, S. Kyritsis, and G. Papadakis, "Comparative thermodynamic study of refrigerants to select the best for use in the high-temperature stage of a two-stage organic Rankine cycle for RO desalination," *Desalination*, vol. 243, no. 1, pp. 74–94, 2009.

[14] B. F. Tchanche, G. Papadakis, G. Lambrinos, and A. Frangoudakis, "Fluid selection for a low-temperature solar organic Rankine cycle," *Appl. Therm. Eng.*, vol. 29, no. 11–12, pp. 2468–2476, 2009.

[15] I. Vaja and A. Gambarotta, "Internal Combustion Engine (ICE) bottoming with Organic Rankine Cycles (ORCs)," *Energy*, vol. 35, no. 2, pp. 1084–1093, 2010.

[16] J. Kalina, "Integrated biomass gasification combined cycle distributed generation plant with a reciprocating gas engine and ORC," *Appl. Therm. Eng.*, vol. 31, no. 14, pp. 2829–2840, 2011.

[17] W. Mingshan, F. Jinli, M. Chaochen, and D. S. Noman, "Waste heat recovery from heavy-duty diesel engine exhaust gases by medium temperature ORC system," *Sci. China Technol. Sci.*, vol. 54, no. 10, pp. 2746–2753, 2011.

[18] H. Tian, G. Shu, H. Wei, X. Liang, and L. Liu, "Fluids and parameters optimization for the organic Rankine cycles (ORCs) used in exhaust heat recovery of Internal Combustion Engine (ICE)," *Energy*, vol. 47, no. 1, pp. 125–136, 2012.

[19] T.-C. Hung, D.-S. Lee, and J.-R. Lin, "An Innovative application of a solar storage wall combined with the low-temperature organic rankine cycle," *Int. J. Photoenergy*, no. 239137, p. 12, 2014.

[20] V. Zare, "A comparative exergoeconomic analysis of different ORC configurations for binary geothermal power plants," *Energy Convers. Manag.*, vol. 105, pp. 127–138, 2015.

[21] E. D. Kerme and J. Orfi, "Exergy-based thermodynamic analysis of solar driven organic Rankine cycle," *J. Therm. Eng.*, vol. 1, no. 5, pp. 192–202, 2015.

[22] F. Calise, M. D. D'Accadia, A. Macaluso, A. Piacentino, and L. Vanoli, "Exergetic and exergoeconomic analysis of a novel hybrid solar–geothermal polygeneration system producing energy and water," *Energy Convers. Manag.*, vol. 115, no. 1–336, pp. 200–220, 2016.

[23] H. Jouhara and M. A. Sayegh, "Energy Efficient Thermal Systems and Processes," *Therm. Sci. Eng. Prog.*, vol. 7, no. 125–130, pp. 1–5, 2018.

[24] A. Fontalvo, J. Solano, C. Pedraza, A. Bula, A. Gonzalez Quiroga, and R. Vasquez Padilla, "Energy, Exergy and Economic Evaluation Comparison of Small-Scale Single and Dual Pressure Organic Rankine Cycles Integrated with Low-Grade Heat Sources," *Entropy*, vol. 19, no. 10, p. 476, 2017.

[25] G. Li, "Organic Rankine cycle performance evaluation and thermoeconomic assessment with various applications part I: Energy and exergy performance evaluation," *Renew. Sustain. Energy Rev.*, vol. 53, pp. 477–499, 2016.

[26] G. Angelino, M. Gaia, and E. Macchi, "A review of Italian activity in the field of organic Rankine cycles," *VDI. Ber.*, no. 539, pp. 465–482, 1984.

[27] B. Saleh, G. Koglbauer, M. Wendland, and J. Fischer, "Working fluids for low-temperature organic Rankine cycles," *Energy*, vol. 32, no. 7, pp. 1210–1221, 2007.

[28] T. Chen, W. Zhuge, Y. Zhang, and L. Zhang, "A novel cascade organic Rankine cycle (ORC) system for waste heat recovery of truck diesel engines," *Energy Convers. Manag.*, vol. 138, pp. 210–223, 2017.

[29] M. J. Moran, H. N. Saphiro, D. D. Boettner, and M. B. Bailey, *Fundamentals of Engineering Thermodynamics*. Wiley, 2011.

[30] S. Quoilin, R. Aumann, A. Grill, A. Schuster, V. Lemort, and H. Spliethoff, "Dynamic modeling and optimal control strategy of waste heat recovery Organic Rankine Cycles," *Appl. Energy*, vol. 88, no. 6, pp. 2183–2190, 2011.

[31] E. Wang, Z. Yu, H. Zhang, and F. Yang, "A regenerative supercritical-subcritical dual-loop organic Rankine cycle system for energy recovery from the waste heat of internal combustion engines," *Appl. Energy*, vol. 190, pp. 574–590, Mar. 2017.

[32] "'Mathworks, «Matlab. Computer Program. MATLAB 2018b»'.".

[33] M. O. Lemmon, E.W., Huber, M.L., McLinden, "NIST Standard Reference Database 23: Reference Fluid Thermodynamic and Transport Properties (REFPROP) - Version 8.0," *Natl. Inst. Stand. Technol. See https//www.techstreet.com/standards/nist-refprop-8-0?product_id=1696006*, 2013.

[34] C. G. F. Val and S. O. Jr, "Deep Water Cooled ORC for Offshore Floating Oil Platform Applications," vol. 20, no. 4, pp. 229–237, 2017.

[35] A. B. Trindade *et al.*, "Advanced exergy analysis and environmental assessment of the steam cycle of an incineration system of municipal solid waste with energy recovery," *Energy Convers. Manag.*, vol. 157, pp. 195–214, 2018.

[36] R. Scaccabarozzi, M. Tavano, C. M. Invernizzi, and E. Martelli, "Comparison of working fluids and cycle optimization for heat recovery ORCs from large internal combustion engines," *Energy*, 2018.

[37] B. Kölsch and J. Radulovic, "Utilisation of diesel engine waste heat by Organic Rankine Cycle," *Appl. Therm. Eng.*, vol. 78, pp. 437–448, 2015.

[38] R. S. El-emam and I. Dincer, "Exergy and exergoeconomic analyses and optimization of geothermal organic Rankine cycle," vol. 59, 2013.

[39] A. Uusitalo, J. Honkatukia, T. Turunen-Saaresti, and J. Larjola, "A thermodynamic analysis of waste heat recovery from reciprocating engine power plants by means of Organic Rankine Cycles," *Appl. Therm. Eng.*, vol. 70, no. 1, pp. 33–41, 2014.

[40] Y. Feng, Y. Zhang, B. Li, J. Yang, and Y. Shi, "Comparison between regenerative organic Rankine cycle (RORC) and basic organic Rankine cycle (BORC) based on thermoeconomic multi-objective optimization considering exergy efficiency and levelized energy cost (LEC)," vol. 96, pp. 58–71, 2015.

[41] N. A. Lai, M. Wendland, and J. Fischer, "Working fluids for high-temperature organic Rankine cycles," *Energy*, vol. 36, no. 1, pp. 199–211, 2011.

[42] N. B. Desai and S. Bandyopadhyay, "Process integration of organic Rankine cycle," *Energy*, vol. 34, no. 10, pp. 1674–1686, 2009.

[43] R. Rayegan and Y. X. Tao, "A procedure to select working fluids for Solar Organic Rankine Cycles (ORCs)," vol. 36, 2011.

[44] Z. Guzovi, "The comparison of a basic and a dual-pressure ORC (Organic Rankine Cycle): Geothermal Power Plant Velika Ciglena case study," vol. 76, no. 2014, 2015.

[45] V. Minea, "Power generation with ORC machines using low-grade waste heat or renewable energy," vol. 69, 2014.

[46] H. Nami, F. Mohammadkhani, and F. Ranjbar, "Utilization of waste heat from GTMHR for hydrogen generation via a combination of organic Rankine cycles and PEM electrolysis," vol. 127, pp. 589–598, 2016.